Petroleum and Coal

Article **Open Access**

2-D Electrical Resistivity Imaging of Bedrock Fissures in Oru, South-West Nigeria: Implications to Stability Integrity for Proposed Engineering Structures

Sakirudeen Akinola Ishola

Department of Earth Sciences, Olabisi Onabanjo University Ago-Iwoye, P.M.B 2002, Ago-Iwoye, Ogun State, Nigeria

Received July 31, 2025; Accepted January 19, 2026

Abstract

Electrical Resistivity Tomography (ERT) is a significant geophysical imaging technique for delineating the presence of fissures in bedrock necessary for evaluating the integrity of engineering structures with a view to examining the trend of suspected bedrock fissures and assessing the vulnerability of structures in the vicinity to potential failure. A total of ten (10) 2-D Electrical Resistivity Tomography (ERT) profile lines were carried out on a length of 115 m using Wenner electrode configuration with Allied Ohmega System Resistivity meter with an initial electrode spacing of 5m and expansion factor n varying between 1 to 5 along each profile, ensuring the surveys were repeatedly done to make up a five level survey. The acquired 2-D data were processed using the ZONDRes2D resistivity package to generate 2D resistivity sections beneath the traverses. The pseudo-section of the inversion results delineated 4 to 11m thick overburden, typically clay and clay-sand, weathered horizons, clay/sandy-clay layers, highly and partially weathered rocks, and fresh bedrock with corresponding resistivity signatures ranging from 20 to 138 Ωm, 25 to 342 Ωm, 327 to 834 Ωm, and 1004 to 1499 Ωm. The regions exhibiting very low resistivity values (< 200 Ωm) were inferred to be zones of suspected fissures. The width of the delineated features ranged from 5 to 30m wide and occurred at depths ranging from 6m to>25m beneath the traverses. Therefore, risks associated with construction on this terrain can be minimized and the long-term stability and ultimate safety of lives and structures can be ensured by adhering to the outputs and recommendations.

Keywords: *2-D Resistivity; Oru-Ijebu; Suspected fissures; Pseudo-section; Fresh bedrock.*

1. Introduction

Over the years, there have been reported increases in the integration of geophysical techniques to investigate different types of construction works and civil engineering-related problems in different parts of the world [1-8]. Some of the problems arising from civil engineering projects include the collapse of buildings and bridges due to distress in their foundations, persistent failures of road pavement sections, and anomalous seepage from engineering structures. Poor engineering designs that are more often than not precipitated by underlying subsurface geological structures, principally fissures [9-11]. Fissures in bedrock are cracks or fractures that occur in solid rock formations. These fissures can significantly impact engineering structures by compromising their stability, causing damage, and potentially leading to catastrophic failure [12-15]. Fissures in bedrock are essentially breaks in the continuity of the bedrock, ranging in size and depth. They can be caused by various geological processes through tectonic activities that create fissures by earthquake and fault movement as the earth shifts and fractures; groundwater depletion through its excessive pumping can cause the land above to compact and settle leading to fissures [16-18]; underground mining activities can voids and instability in the surrounding bedrock, leading to surface subsidence and fissuring [17]; over time, natural processes like erosion and weathering can weaken the bedrock and cause fissures to develop [15–16]. Fissures in bedrock can pose serious threats and destructive implica-

tions to engineering structures in several ways; fissures can undermine the stability of foundations leading to settlement, tilting, and even collapse of buildings, bridges and other engineering structures [19-20], fissures can enhance the risk of slope failure by acting as pathways for water infiltration, weakening of the soil and rock masses thereby increasing the risk of landslides and slope failures [21], fissures can cause ruptures in underground utilities leading to leaks of water, gas or other materials as well as damage to pipelines, electrical and communication lines [16,20-21], fissures can reduce the bearing capacity of the soil and rock mass, making it difficult to support heavy structures [22-23], fissures have been found to amplify seismic waves during earthquakes thereby increasing the risk of damage to structures built on or near them [24-26], fissures can provide pathways for contaminants to enter groundwater potentially affecting the quality of drinking water supplies [27-28]. The resultant effects of these implications can cause roads to buckle and crack, and bridges to become misaligned or damaged; buildings can experience foundation problems, including settlement, cracking, and even collapse due to fissures in the underlying bedrock; fissures can compromise the structural integrity of dams and reservoirs, potentially leading to catastrophic failures [29-41].

The presence of fissures in bedrock has long been recognised to underplay the integrity of engineering structures [42-45]. They function as a conduit through which groundwater seeps into bedrock and partly consolidated deposits. Waterlogged marshy environments have most times been discovered to be underlain by fissured bedrock [46-48]. The destructive implications of the presence of fissures to civil engineering structures cannot be overlooked.

The electrical resistivity method has been utilised to delineate bedrock fissures with recordable success in the past years due to its cost-effectiveness and time-saving considerations [49-51]. Sangodiji *et al.* [52] undertook a geophysical investigation of foundation failure of the distressed former building of Ogbomoso North Local Government Secretariat using Electrical Resistivity method involving Vertical Electrical Sounding (VES) and Electrical Resistivity Tomography (ERT) techniques. A 20-30cm wide fracture zone trending in the NE-SW direction was consequently delineated around the distressed building. Though the failure of the building foundation was suspected to have been precipitated by differential settlement within the suspected faulted zone, the lateral extent and complete orientation of the delineated fault zone could not be ascertained by the study due to the insufficient number of traverses established around the area. Akinlabi *et al.* [11] later conducted 2D-ERT surveys around the site of the failed Ogbomoso North Local Government Secretariat building to examine trends in suspected bedrock features and assess the vulnerability of nearby structures to potential failure. 5 to 20cm wide bedrock fissures at depths ranging from 5m to >25m were delineated; the incessant road failures and groundwater seepages observed within the study area were attributed to the presence of network of bedrock fissures. Also, a geophysical survey comprising the electrical resistivity method utilising VES and ERT was undertaken around southern Ilesa, southwestern Nigeria by [53] with the aim of studying the structural defects which may be responsible for future problems. The results of the study revealed that the causes of the observed cracks and distress on the walls within the site might have been influenced by the differential settlement resulting from the incompetent subsoil materials and the fractured bedrock on which the foundation of the building was laid.

The increase in varying categories of residents in Oru and its environs most notably students, staffs, artisans in the study area as a result of proximity to Olabisi Onabanjo University, Ago-Iwoye Permanent sites and the mini-campuses has led to increase in populations and activities like trading to meet the daily needs of the people, construction of residential buildings to provide shelter for the teeming populations, drilling of numerous boreholes to meet the water demands of the people and the need to construct more feeder roads to link other neigbouring towns like around Oru, Awa, Ilaporu, Ijebu-Ode, Ijebu-Igbo, Omu, Ilishan among others. The increase in disposed water and poor drainage systems in Oru and adjoining areas make the area waterlogged, particularly during the rainy season. Water erodes pavement edges, which, if left unchecked, will result in the underscoring of the pavement, ultimately leading to the collapse of the surface structure. Water seeps into cracks of the asphalt surface of the existing road and slowly erodes the subsurface which ultimately creates subterranean

crates that eventually lead to potholes and to a more extreme extent; sinkholes. When the cracks and potholes are not properly addressed, sinkholes would open up, but if the subsurface is well designed where water is allowed to properly drain off the sides, even in the torrential downpour, the section of the road would be found dry. In the past, roads in Oru and its environs have been occupied with only bicycles, light cars, light pick-ups trucks and motorcycles and tricycles but today due to the increased economic, social, and educational activities, these areas are now fully occupied with full size 18 wheelers trucks and trailers alongside the aforementioned lighter vehicles. The difference here is about weight, and vehicles plying local roads that exceed the weight limits of the roads may gradually lead to road failure. Artificial materials beneath the subsurface, like drainage structures, pipes, manholes, cables, can result in the emergence of asphalt patches, asphalt humps across the constructed road, which may inevitably lead to that section of road being crumbled into pieces, leading to potholes, standing water and eventually a collapse of million-dollar projects. The growing demand for new feeder roads and site development necessitates more site investigations to identify potential subsurface defects and avoid the unpleasant experience of road and building failures. Geophysical investigations are very significant in evaluating the physical properties of the subsurface in terms of its soil type, soil competence, soil corrosivity, depth to bedrock and lithological sequence. Site engineers sometimes fail to incorporate pre-construction investigations into their job schedules due to cost and other considerations, such as assumptions in structural design. A geophysical investigation is therefore necessary at the site to identify potential future subsurface issues and propose solutions before the erection of a building or the construction of roads. Therefore, this study shall go a long way as means of delineating the potential fissures as well as for mitigation and prevention of fissures in the study area through which a thorough site investigations including geological, geophysical and geotechnical surveys, potential fissure hazards can be identified before construction [41,54-56]; engineering should be designed to withstand the potential impacts of fissures using appropriate foundation systems and construction techniques; management of groundwater levels can assist in preventing land subsidence and fissure formation in areas prone to these issues [12,15]; slope stabilization measures such as retaining walls and drainage systems can be adopted in mitigating the risk of landslides and slope failures in fissure prone areas [12,15,57]; regular monitoring and maintenance of structures built on or near fissures can help identify and address potential problems early on [57-60].

2. Study area

2.1. Physiography and accessibility

The study area lies within Oru-Ijebu. It is located between latitude 6°57'19"N and longitude 3°56'31"E. The area is accessible through major and minor roads, linking Oru-Ijebu with several towns and localities including Ago-Iwoye, Awa, Ilaporu, Imope and Ijebu Igbo and it lies within the basement complex of Southwestern Nigeria [61-62]. The relief is moderately low forming ridges in some places an undulated plain dotted with small isolated hills or hilly rocks are noticed generally within Ago−Iwoye with the coverage extent of 10.5km^2. The highest elevation is 200m with most of the outcrops being moderately high and some relatively flat. The general level of surface rises Northwards from about 0-500ft above the coast northward to the area of the crystalline rocks. Drainage pattern is predominantly dendritic. The study area falls within the equatorial belt giving the area two major seasons namely, the wet and dry seasons. The climate is characterized by annual average minimum and maximum temperatures of 23°C and 35°C respectively, and it experiences double maximal rainfall, with the peak between June and September [63-64]. The months of December and January are relatively dry in the Oru community. Before the first rain in late March or early April, the weather is humid, with humidity around 50% year-round [65-66]. The dry season is rather short with very hot days. In a year, the maximum rain is recorded between June and October in this area. The vegetation of the mapped area indicates that it lies within the tropical rainforest of Nigeria, with many light forests, scattered cultivations, and scrub [66].

2.2. Geological setting

The study area, Oru and its environs, lies within the Basement Complex of south western Nigeria. It forms part of the Pan African mobile belt which lies to the east of West African Craton. Hence, several authors have worked on and classified the basement rocks based on their association and geochronology. Some of the classifications were carried out by [67-68]. [69] classified the basement complex rock units into 5 different groups viz: the migmatite-gneiss-quartzite complex, the newer metasediments, Chanockite, diorite and gabbro, older granite, Unmetamorphosed acid and basic intrusive and hyperbyssal rocks. The major rock types in the area of study include granite gneiss, granite, banded gneiss, pegmatite and undifferentiated migmatite and these have been intruded by quartz veins and pegmatite veins. (Figure 1). Granite gneiss is the major rock that dominated the study area. It belongs to the gneiss group. There is a considerable variation in the amount of mafic and felsic minerals. They are typically medium grained in texture and the minerals present include quartz, biotite, plagioclase, orthoclase and other mineral accessories. Granite gneiss stretches from the eastern part to the north-west of the area. Generally, it is grey in colour and texturally medium-grained. Mineralogically, it consists of quartz, plagioclase, feldspar, biotite and hornblende. Granite is the second most abundant rock type in the area covering the entire eastern and northwestern region. The colour is grey, and the texture is medium-grained. Banded Gneiss is foliated, and the rocks consist of alternating bands of light and dark minerals. The light band is composed of felsic minerals, mainly quartz and feldspar, while the dark band consists of mafic minerals. Mineralogically, banded gneiss contains both felsic and mafic minerals [70]. Pegmatite is located in the western part of the study area. The entire Oru Township is underlain by pink pegmatite. Pegmatite is a very coarse-grained minor igneous rock; it is formed from the residual magma that is rich in volatile and fugitive elements. They occur as a massive intrusion in Oru. Texturally, it ranges from medium to coarse-grained. Mineralogically, feldspar, mica (muscovite dominating over biotite) and quartz are the most abundant minerals, while muscovite and tourmaline occur as accessory minerals. Muscovite flakes from the weathered pegmatite litter the immediate (Figure 1).

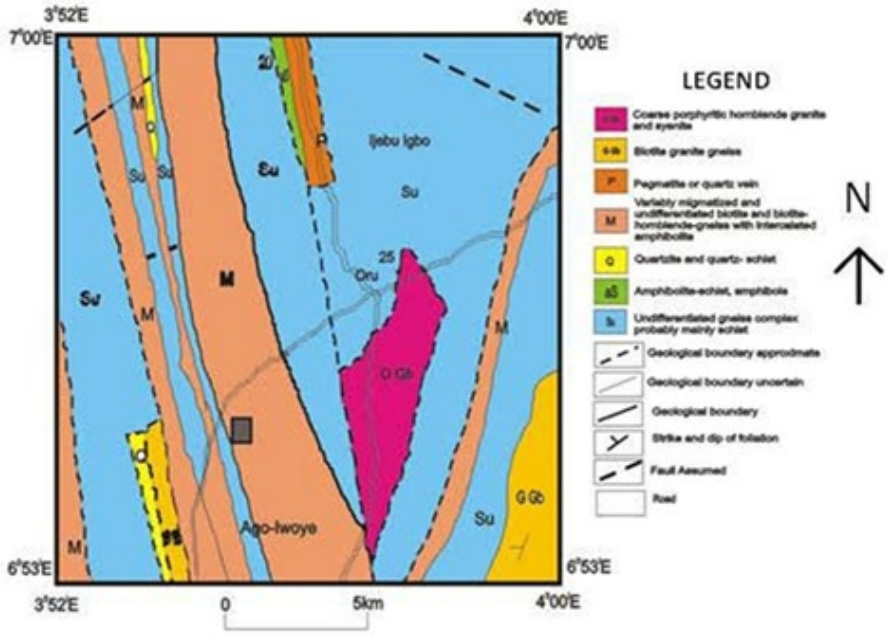

Figure 1. Geological map of the study area (modified after [71]).

These types of aquifers are superimposed or isolated. In a crystalline medium, capacitive and conductive functions both exist within each aquifer. The potentials of these aquifers depend on hydrological balance parameters and their configurations. Water-bearing fissures and

fractures; tectonics is the major factor governing water flow in the study area. Figure 1 shows the geological map of the study area [71]; Figure 2 shows the physiography and accessibility map of the study area, and Figure 3 shows the data Acquisition map of the study area, with points of 2D profiles along each traverse line, and Figure 4 is the image map showing points of 2D profiles on Google Earth satellite imagery.

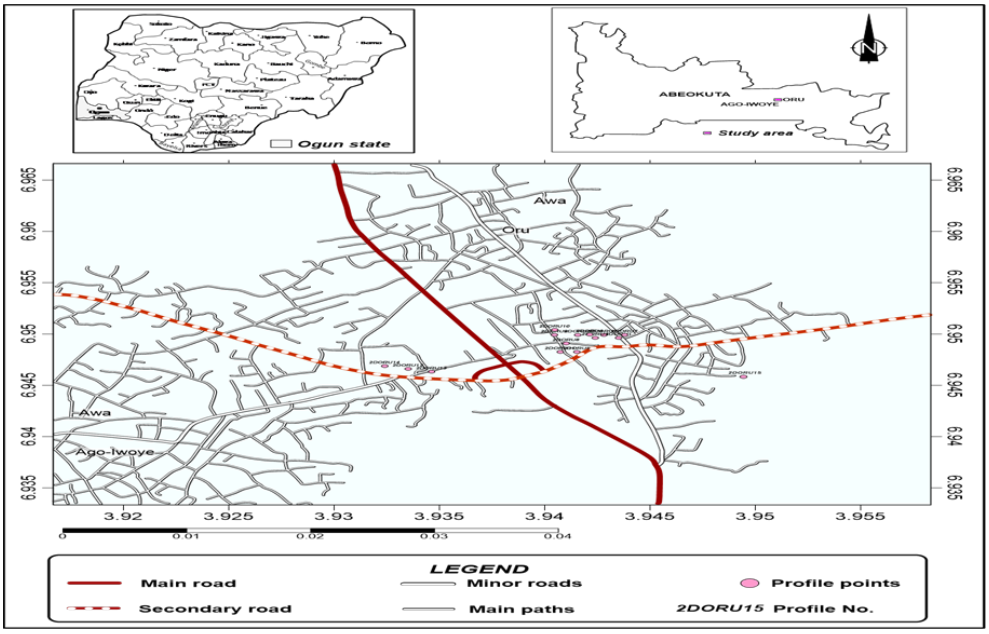

Figure 2. Location and accessibility map of the study area (modified after [66]).

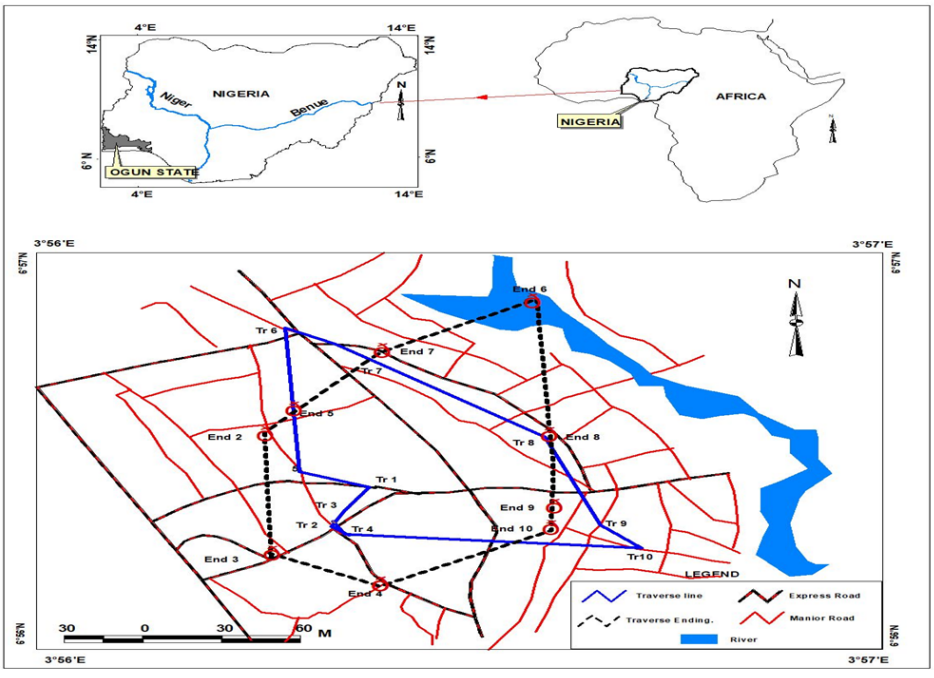

Figure 3. Data acquisition map showing points of 2D profiles along each traverse line.

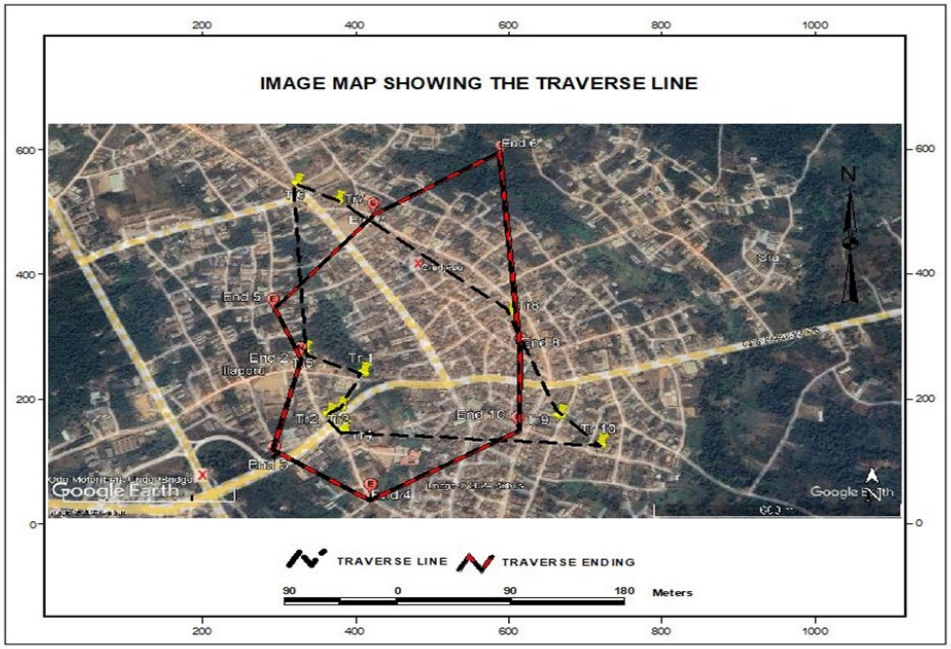

Figure 4. Image map showing 2D profiles of the study area in Google Earth satellite imagery.

3. Materials and methods

2-D Electrical Resistivity Imaging Techniques were employed in this study to measure changes in Earth's resistivity both vertically and horizontally due to the complex geology of the study area. Electrical resistivity is a function of porosity, fluid saturation, resistivity of the pore fluid and the solid, and the material texture, among others. A conductive body concentrates electric current flow lines towards itself, while a resistive body causes the current to flow around itself. Electrical resistivity imaging is a survey technique developed for investigating areas of complex geology where resistivity sounding and other techniques are unsuitable [72]. In this study, a preliminary survey was conducted at the investigated locations, which involved reviewing previous work and acquiring topographic and geologic maps of the area. The terrain was examined for topographic effects, specifically sharp elevation contrasts along a chosen profile. 2-D electrical resistivity imaging data were acquired along ten (10) parallel traverses using Allied Ohmega system resistivity meter. The Wenner electrode configuration was adopted, with the current and potential electrodes spaced 5 m apart, given the available space. The profile length on each profile were 115 m long, with an initial electrode spacing of 5m, 10 m, 15 m, 20 m and final spacing of 25 m along each profile ensuring the surveys were repeatedly done to make up a five level survey (n = 1, 2, 3….5) and (na = 5, 10, 15,…25 m) (Figure 3). All stations were georeferenced using the Geographic Positioning System (GPS) for accuracy. The resulting resistance values were multiplied by each array geometric factor to obtain apparent resistivity values, which were then processed in ZONDRES 2D software to generate 2D resistivity inversion sections along the traverses. The inversion was consequently performed to generate the electric resistivity structure of the subsurface and qualitatively interpreted to reveal possible bedrock fissures in the area.

4. Results and discussion

The 2D resistivity reveals the vertical and lateral subsurface resistivity distribution beneath the study area, displayed as inverted sections, which depict overburden rock materials, typically clay, underlain by fresh bedrock. Within the context of this study, overburden refers to formation materials overlying the fresh bedrock, which comprises the topsoil, weathered layer, and presumably the partly weathered bedrock. Apparently, there is no clear demarcation or

boundary line between the topsoil and the weathered layer. The bedrock is inundated with weak zones and characterized by low resistivity suspected to be fissures which must have been precipitated by intense tectonic activities in the area [11,73]. Detailed descriptive analyses of resisti vity sections for each 2D profile beneath the traverses are hereby presented (Figures 5 to 14).

Image Traverse Line 1: The 2D resistivity sections beneath traverse 1 reveal overburden with resistivity ranging from 20 to 76.6 Ωm and thickness varying from 3 m to 7 m. The exhibited low resistivity values represent the bedrock underlying the extreme southwest portion of the traverse, which appears to be partly weathered with resistivity of 220 Ωm at a lateral distance of 50 to 102 m. The low resistivity zone of 20 Ωm observed at a lateral distance of 20 to 42m are suspected to be bedrock fissures found beneath 4m and extended to 25m in depth (Figure 5).

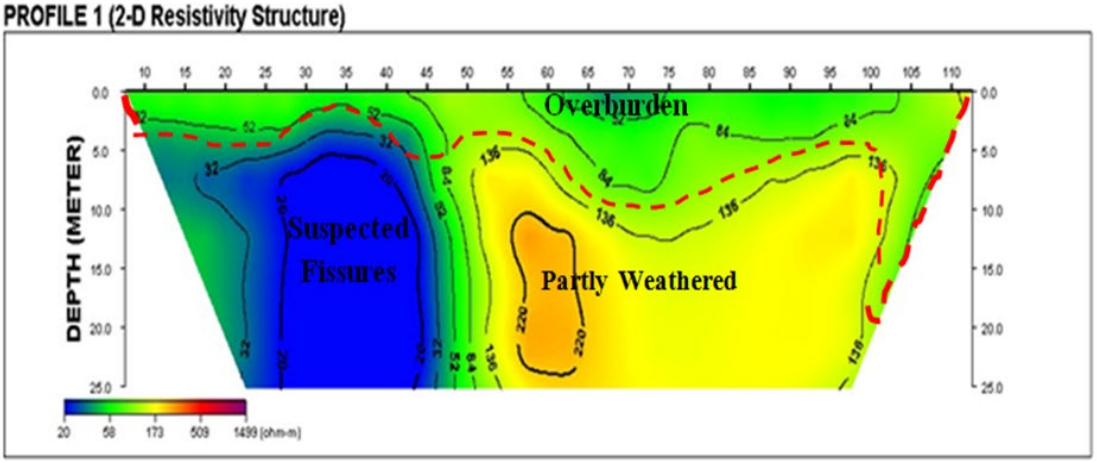

Figure 5. Oru 2-D profile 1 showing the 2D resistivity section beneath traverse 1.

Image Traverse Line 2: The 2D resistivity section beneath traverse 2 is underlain by a thick overburden that ranged from 4 m to 15 m with resistivity ranging from 20 to 135 Ωm. The exhibited very low resistivity zone was delineated at a lateral distance of 0 to 63m from the surface to a depth of 9 m, representing clay and clayey sand. Underlying the extreme southwest portion of the traverse is a relatively resistive overburden of about 15m thick with resistivity of 84 to 345 Ωm, which appears to be partly weathered at a lateral distance of 48 to 115 m. The low resistivity zone around 20Ωm observed at a lateral distance of 65 to 95 m are suspected to be bedrock fissures found beneath 10m and extended to 25 m in depth (Figure 6). The resistivity of the fresh bedrock ranged from 1001 to 1499 Ωm. The more resistive overburden must have been propelled by the suspected fissures of bedrock occurring within the delineated interval [74-75].

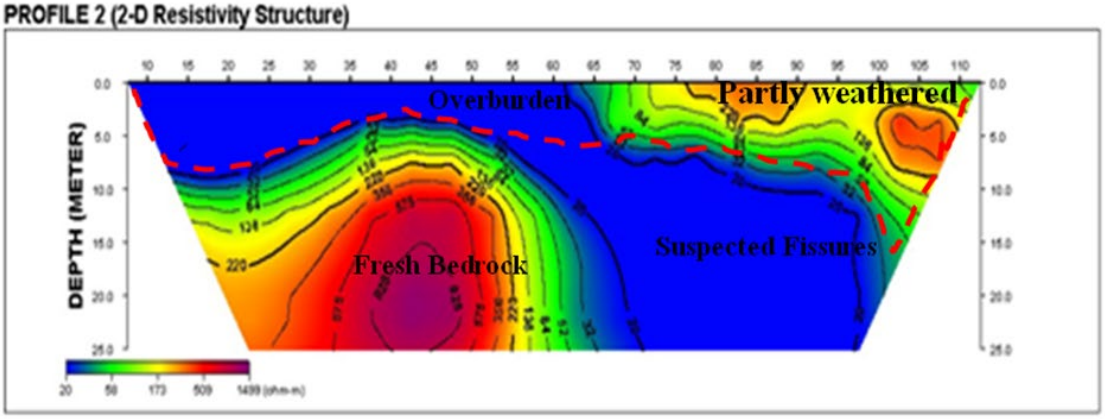

Figure 6. Oru 2-D profile 2 showing the 2D resistivity section beneath traverse 1.

Image Traverse Line 3: The 2D resistivity sections beneath traverse 3 possess an overburden of resistivity value range of 23 to 341 Ωm and thickness varying from 2 m to 10 m suggestive of clayey sand mixtures. The bedrocks underlying this layer were partly weathered with resistivity of 135 to 625 Ωm at lateral distances of 0 to 25m, 43 to 68 m and 78 to 92 m at corresponding depths of 25, 25 and 6 m, respectively. Two lower-resistivity zones were observed at lateral distances of 30 to 40 m and 70 to 85 m, and were delineated as weak zones. These weak zones were suspected to be of bedrock fissures beneath 10m and extended to the end of the section (Figure 7).

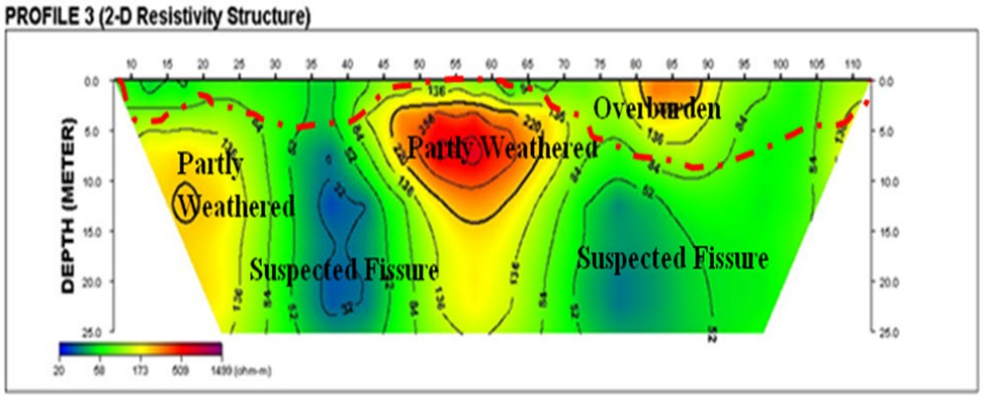

Figure 7. Oru 2-D profile 3.

Image Traverse Line 4: The 2D resistivity section beneath traverse 4 is underlain by a thick overburden of about 6 m with resistivity ranging from 50 to 84 Ωm consisting of clayey sand at a varying lateral distance of 11 to 45 m, 50 to 60 m, 75 to 80 m, and 85 to 90 m. This was underlain by a partially weathered zone of 136 to 420 Ωm at a lateral distance of 50 to 70 m, 82 to 115 m to a depth of 27 m with a thickness of 12 m. The exhibited very low resistivity zone was delineated at a lateral distance of 45 m to 115 m from the depth of 45 m to 70 m, suspected be fissures of bedrock occurring within the delineated intervals [48,75].

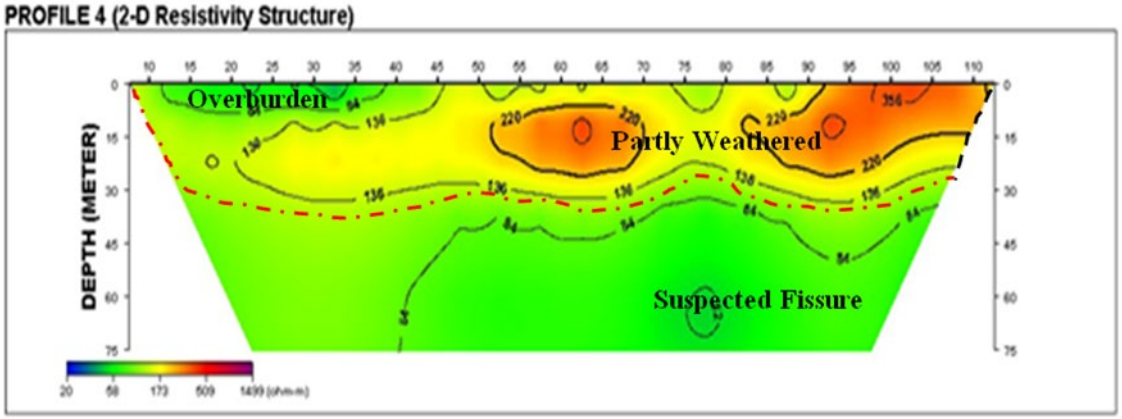

Figure 8. Oru 2-D profile 4.

Image Traverse Line 5: The 2D resistivity section was very similar to traverse 4; underlain by an overburden of about 4 m with resistivity ranging from 38 to 93 Ωm consisting of a clayey sand mixture at a varying lateral distance of 11 to 44 m, 50 to 57 m, 73 to 80 m, and 85 to 88 m. This was also underlain by a partially weathered zone of 136 to 356 Ωm at a lateral distance of 50 to 70 m, 82 to 115 m to the depth of 10 m with a maximum thickness of 7 m. The exhibited very low resistivity zone was delineated at a lateral distance of 45 m to 115 m from a depth of 13 m to 25 m, which is suspected to be characterised by a bedrock fissure within the delineation interval in Figure 9.

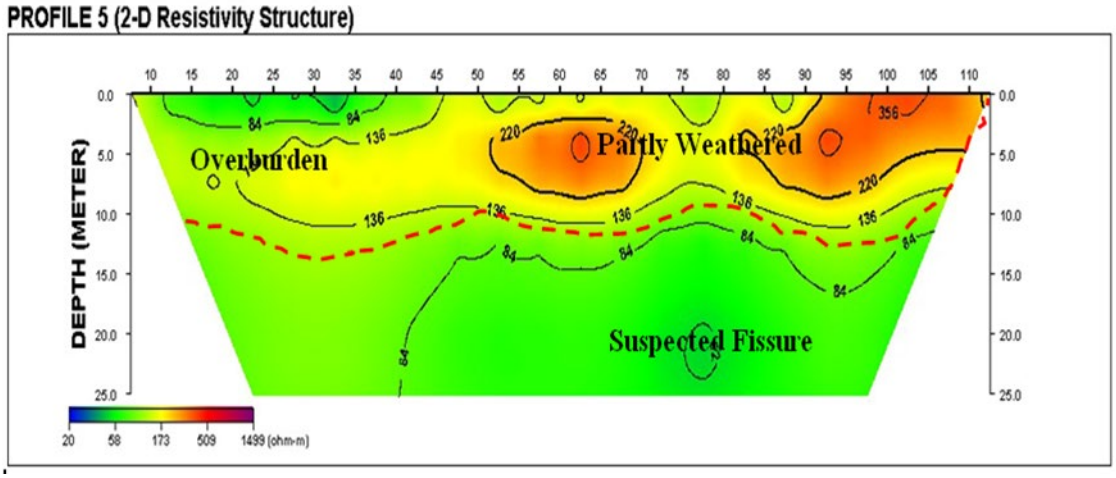

Figure 9. Oru 2-D profile 5.

Image Traverse Line 6: The 2D resistivity section beneath traverse 6 at the northeast of the study area underlain by overburden varying from 3 m to 7 m with observed low resistivity 20 to 84 Ω m consisting of clayey-sand mixture varying lateral distance of 45 to 50 m, 85 to 90 m with the clay exhibiting a lower resistivity of 32 Ωm with a very thin bed of 1.5 m. This was also underlain by a partially weathered zone with resistivity values of 220 to 575 Ωm at a lateral distance of 25 to 50 m, while the highly weathered zone exhibited resistivity values of 84 to 136 Ωm with a maximum thickness of 17 m. The weathered horizon extended to a total depth of 20m. Two separate zones of significantly low resistivity values (≤ 20 Ωm) were observed between the partly weathered horizons and were consequently delineated as suspected fissures (Figure 10).

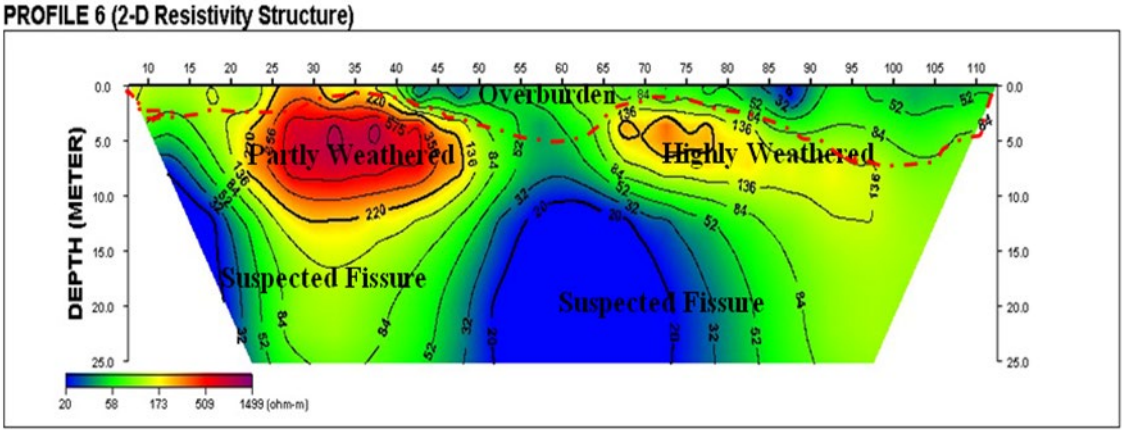

Figure 10. Oru 2-D profile 6.

Image Traverse Line 7: The 2D resistivity section beneath traverse 7 was underlain by an overburden of resistivity values ranging from 52 to 84 Ωm at varying depths of 2 to 8 m.

Clay-sand was found at a near-surface at lateral intervals of 30 to 45 m on a thin overburden around 1.5 m. A partially weathered zone was also delineated within a lateral distance of 65 m to 95 m with a thickness of about 5 m, while a highly weathered zone at a lateral interval of 45 to 60 m was also delineated with continuous extension from the depth of 4 m to 25 m (Figure 11). Between the highly weathered zone and beneath the partly weathered zone, two anomalous zones observable at lateral intervals of 10 to 15 m and 70 to 80 m within the bedrock are suspected to be weak or distressed zones occasioned by fissuring. Also, the more resistive overburden observed as overlying formation rock materials must have been propelled by the suspected fissures of bedrock occurring within the delineated interval [11,48].

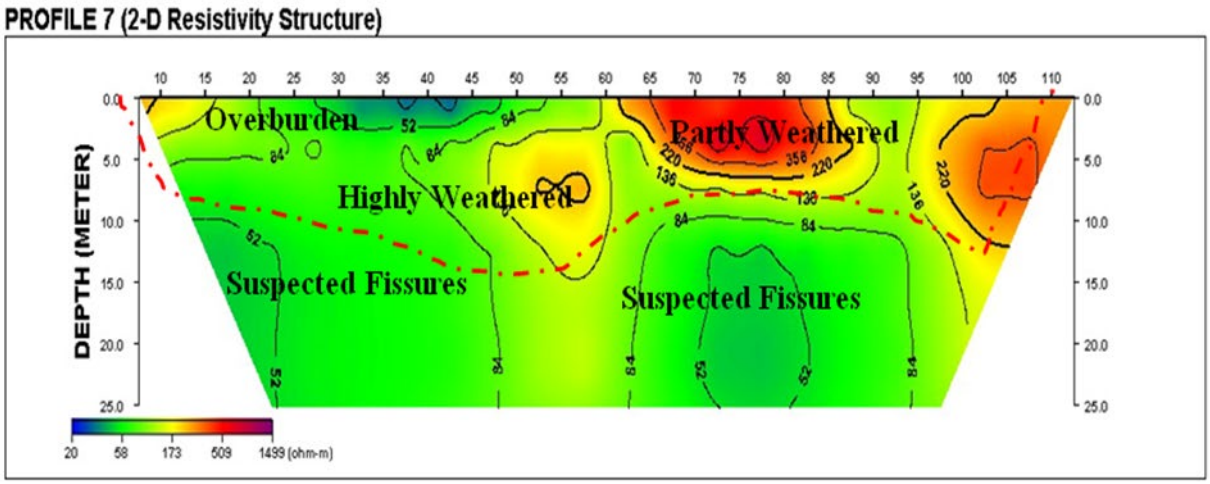

Figure 11. Oru 2-D profile 7.

Image Traverse Line 8: The 2D resistivity section beneath traverse 8 was underlain by overburden of resistivity values ranging from 52 to 84 Ωm at varying depths of 2 to 9 m. Small portion of clay-sand materials were found at a near-surface at lateral intervals of 0 to 20m on a relatively thin overburden up to the depth of 3 m. Highly weathered zones were delineated within a lateral distance of 37 m with continuous extension throughout the entire length of the section, with accompanied varying thickness of 5 m (depth of 5 m to 10 m), while the extension of the highly weathered zone continuously runs to merge with the fresh bedrock. The delineated low resistivity zone between the distances of 25 m to 66 m was suspected to be weak zones cutting deep into the basement (Figure 12).

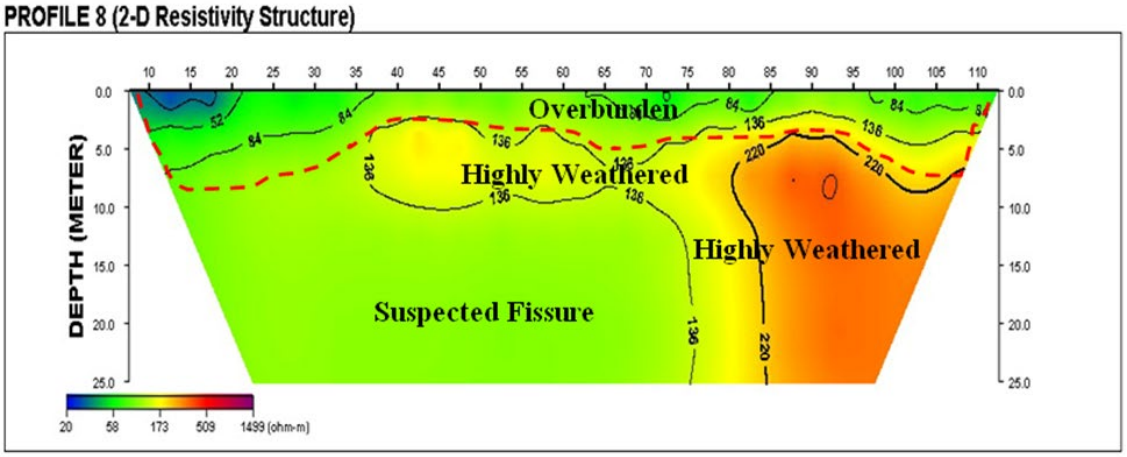

Figure 12. Oru 2-D profile 8.

Image Traverse Line 9: The 2D resistivity section beneath traverse 9 was underlain by overburden of resistivity values ranging from 38 to 52 Ωm at varying depths of 5 to 12 m. Small portion of Clay-sand materials were found at a near-surface at lateral intervals of 20 to 35 m on a relatively thin overburden up to the depth of 3 m. Partially weathered zone was delineated at a lateral distance of 55 m to 115 m with continuous extension to the end of the section, with a thickness greater than 15 m as the extension of depth of the highly weathered zone merges with the fresh bedrock of the area. The delineated low resistivity zone observed between the lateral distances of 30 m to 47 m was suspected to be a weak zone that emerged from a depth of 5 m and continuously moved into the basement depth into the basement (Figure 13).

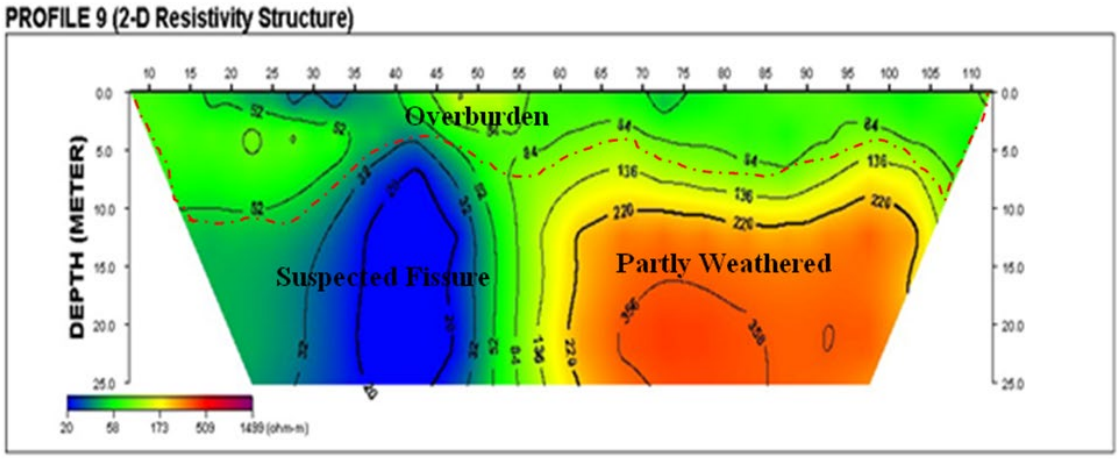

Figure 13. Oru 2-D profile 9 .

Image Traverse Line 10: The 2D resistivity section beneath traverse 10 was underlain by an overburden of resistivity value range of 52 to 84 Ωm at varying depths, with minimum and maximum thickness of 2 and 11 m, respectively. Partially weathered zone was delineated at a lateral distance of 60 m to 115 m with continuous extension to the end of the section, with a thickness greater than 17 m as the extension of depth of the highly weathered zone merges with the fresh bedrock of the area. The delineated low resistivity zone observed between the lateral distances of 30 m to 50 m was suspected to be a weak zone that emerged from the depth of 5 m and continued deeply into the fresh bedrock (Figure 14).

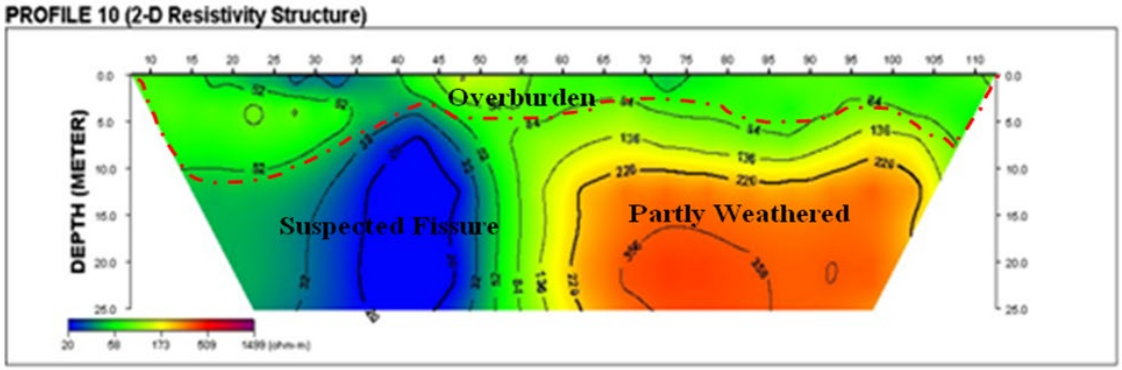

Figure 14. Oru 2-D profile 10.

The lateral and vertical variation of resistivity signatures established in the study area generally reveals overburden with corresponding resistivity outputs less than 100 Ωm characterized of clay and partly clay-sand materials, which were sometimes less than 25m but progressively became thinner. Highly weathered rocks generally have a lower resistivity compared to partially weathered rocks because weathering reduces the resistivity of rock owing to increased porosity and the presence of conductive materials like water and clay minerals [68, 73-76]. Weathering processes (like chemical alteration, fracturing and increased porosity) break down solid rock materials into smaller particles and consequently create voids; these voids can be filled with water, which is a good conductor of electricity, thus lowering the overall resistivity of weathered materials [73,76-78]. Highly weathered rock has undergone more extensive alteration and has a higher degree of fracturing and porosity than partially weathered rock. This degree of fracturing and porosity is greater than that of partly weathered rock, which leads to a greater abundance of water and conductive materials, resulting in lower resistivity [77-81]. Resistivity values for highly weathered rocks can range from 22 to 345 Ωm while partially weathered rocks

can have resistivity values between 324 to 926 Ωm. Areas of low resistivity signatures suspected to be characterized by features of fissures were delineated. In all the investigated profiles along each traverse, there was no anomalous location with extremely low resistivity ($< 10\Omega m$) resulting from possible water saturation that could have been attributed to a suspected buried channel from which groundwater could accidentally spring up. At present, there is no reported circumstantial field evidence that the bedrock fissures have any noticeable impacts on the foundation of buildings in the existing residential environment in this area, as there are no cracks precipitated by probable settlement.

5. Conclusion

The 2D resistivity section beneath the study area was produced revealing the observed variation of overburden of resistivity values ranging from 20 to 84 Ωm at traverse line 6 to 23 to 341 Ωm at traverse line 3 at varying depths with minimum and maximum thickness of 4 m in traverse line 1, 5, 6 and 11 m in traverse line 2. Locations where the overburdens were characterized by typical clay-sand were fully competent for road construction in their natural state due to the extensive presence of weak layers. Engineering modifications such as soil stabilization, excavation and replacement would be necessary for safe and durable road development. The weathered horizons and fissures delineated in the subsurface geological formations of the study area can significantly affect the stability and longevity of buildings and roads constructed on them, and the network of bedrock fissures can induce groundwater seepages and persistent road failures. Partially and highly weathered zones, along with fissures, can reduce soil strength, increase water absorption and swelling, and cause differential settlement and foundation instability, potentially leading to highway pavement failure and structural damage. These can have huge structural implications on buildings, resulting in cracks in walls and foundations, tilting or sinking of structures and potential collapse. While pavement cracking, potholes, heaving and overall instability of the surface can become common occurrences on roads. Mitigation measures like detailed geophysical investigations by integrating 3D electrical resistivity tomography with seismic refraction surveys, detailed geotechnical analysis using shear strength, compressibility and water absorption, foundation designs with ground improvements, implementations of effective drainage designs, ground improvement methods like compaction, grouting or stabilization and selection of appropriate materials that are resistant to weathering and suitable for the broadened the bearing capacity of the overall site conditions are hereby recommended for the study area if engineering structures are to be erected. Therefore, the outcomes of this study have enhanced understanding of subsurface geologic conditions and the possible impacts of weathering and fissures on the subsurface earth materials in the study area, using 2D electrical resistivity imaging, and have recommended appropriate mitigation measures. Site engineers can minimize the risks associated with construction on this terrain and ensure the long-term stability and sustainability of proposed engineering structures.

Acknowledgement

The author expresses his gratitude to the entire Oru community within the Ijebu North Local Government Area of Ogun State for their permission and assistance.

Conflict of interests

The author declares that there are no contrasting interests, as to the production of this paper.

References

[1] Kowalczyk S, Zawrzykraj P, and Mieszkowski R. Application of Electrical Resistivity Tomography in Assessing Soil Conditions. Geological Q, 2015; 59(1): 367-372. https://doi.org/10.7306/gq.1172

[2] Kowalcyk S, Zawrzykraj P, Maslkowski, M. Application of Electrical Resistivity Method in Assessing Soil Foundation of Bridge Structures: A case study from the Warsaw Environs, Poland. Acta Geodynamics Geomater, 2017; 14(1): 221-234. https://doi.org/10.13168/AGG.2017.0005

[3] Akinlabi IA, and Ayanrinde OS. Geophysical Investigation of Anomalous Seepage in and around Earth Dam Embankment in Ogbomoso, Southwestern Nigeria. International Journal of Scientific and Engineering Research, 2018; 9(7): 1455-1467. https://doi.org/10.35840/2631-5033/1827

[4] Akinlabi I, Akinrimisi OE, and Fabunmi MA. Subsurface Investigation of Landslide using Electrical Resistivity and Self-Potential Methods in Oke-Igbo, Southwestern Nigeria. IOSR Journal of Applied Geology and Geophysics. 2018; 6(5): 67-74. https://doi.org/10.9790/0990-0605016774

[5] Skutnik Z, Badja M, Lech M. Applications of RCPTU and SCPTU with other Geophysical Test Methods in Geotechnical Practice. Hicks, M., Pisano, F., Peuchen, J., Eds; RC Press, London, UK. 2018; 88-92.

[6] Trappe J and Kneisel C. Geophysical and Sedimentological Investigations of Peatlands for the Assessment of Lithology and Subsurface Water Pathways. Geosciences, 2019; 9(118): 78-83. https://doi.org/10.3390/geosciences9030118

[7] Lech M, Skutnik Z, Badga, M, and Markowska-Lech K. Applications of Electrical Resistivity Surveys in Solving Selected Geotechnical and Environmental Problems. Applied Sciences, 2020; 10(7): 2263. https://doi.org/10.3390/appl10072263.

[8] Conclaves JTD, Botelho MAB, Machado SL, Netto LG. Correlation between Field Electrical Resistivity and Geotechnical SPT blow counts at Tropical Soils in Brazil. Environmental Challenges, 2021; 5(1): 1-12. https://doi.org/10.1016/J.ENVC.2021.100220

[9] AZGS. Arizonal Geological Survey. Locations of Mapped Earth Fissure Traces in Arizona (D1-39V.01.29.2015) Tuczon, AZ. Arizonal Geological Survey Digital Information, 2015.

[10] Conway BD. Land Subsidence and Earth Fissures in South-Central and Southern Arizona, USA. Hydrogeology Journal, 2016; 24(3): 649-655. https://doi.org/10.1007/s10040-015-1329-z

[11] Akinlabi IA and Bayowa, OG. 2D Electrical Resistivity Imaging of Bedrock Fissures in Ogbomoso, Southwestern Nigeria. LAUTECH Journal of Civil and Environmental Studies, 2021; 7(2): 46-54. https://doi.org/10.36108/laujoces/1202.70.0250

[12] Chang J, Deng Y and Mu H. Effects of Earth Fissure on the Seismic Response Characteristics of Nearby Metro-stations and Tunnels. Bulletin of Engineering Geology and the Environment. 2023; 82 (232): 1011-1019. https://doi.org/10.12989/eas.2023.24.1.053

[13] CA. Coal Authority and Mining Remediation Authority. Geological Disturbance Fissures and Breaklines Dataset Userguide. 2024. datasolutions@coal.gov.uk

[14] Alsalari A, Nwafor BO, Hermana M, Marzouki A, Hassan HM and Irfan M. Understanding the Mechanisms of Earth Fissuring for Hazard Mitigation in Najiran, Saudi Arabia. MDPI Sustainability Journals. 2025; 15(7): 300-306. https://dx.doi.org/10.3390/su15076001

[15] Zhang C, Zhing W, Chen J, Li X, Pu Y, Yi J and Xu, Y. Response Spectra and Design Specification of Good Fissures sites under Seismic Actions. Scientific Reports. 2025; 15(1): 16120. https://dx.doi.org/10.1038/s41598-025-01036-9

[16] Garcia S, Merlos J and Trejo P. Subsidence and Induced Subsoil Cracking in the Southeastern of Mexico City. Advances in Civil Engineering. 2024; 1(1): 193-1002. https://dx.doi.org/10.1155/adce/6090327

[17] Cao G, Deng, Mu H, Chang J, Xan, Y, and Niu D. Land use sustainability Assessment of the Dynamic Response of Typical Bedrock-Buried-Hill Earth Fissures Sites in the Suxichang Area. MDPI Sustainability Journals. 2025; 16(8): 300-306. https://dx.doi.org/10.3390/su16083117

[18] Liu Y, Peng J, Wang F, Zhu F, Jia Z and He M. Development Mechanism of Rainfall-Induced Ground Fissures in the Kenya Rift Valley.Water. 2025; 14(20): 3215-3221. https://dx.doi.org/10.3390/w14203215

[19] Yan F, Zhi M, and An Y. Revealing Large-Scale Surface Subsidence in Jincheng City's Mining Clusters using MT-INSAR and VMD-SSA-LSM Time Series Prediction Model. Scientific Reports. 2025; 15(5726). https://doi.org/10.1038/s41598-025-88524-0

[20] Zhang, K, Liu S and Van Z. Effects of Underground Mining on Soil-Vegetation System: A Case Study of Different Subsidence Area. Science Partner Journals. Ecosystem, Health, and Sustainability. 2023; 9(1): 445-466. https://dx.doi.org/10.34133/ehs.0122. spj.science.org.

[21] Li W, Zhang J, Wang N, Zhang L, Qiu Q and Zhang H. Experimental Study on Morphological Characteristics of Vertical Fissures Grouting in Earthen Sites. Measurement 2023; 239(1): 422. https://doi.org/10.1016/j.measurement.2024.115537

[22] Peng J, Qiao J, Leng Y, Wang F and Xue S. Distribution and Mechanism of Good Fissures in Wei River Basin, the Origin of the Silk Read. Environmental Earth Sciences. 2016; 75(8): 777-785. https://dx.doi.org/10.1007/s12665-016-5527-3.
[23] Kong Y, Li Z, Sun K, Qi Z and Hu R. Study on the Extension Mechanism of Fissures in Expensive Soil-Based on Fracture Mechanics Test Method. Engineering Geology. 2024; 343(1): 78. https://dx.doi.org/10.1006/j.enggeo.2024.10778.
[24] Liu H, Zhou TT, Liu X, Deng KZ and Lei SG. Factors that Trigger the Development of Mining –Induced Ground Fissures and Standards to Treat them in Shallow Coal Mining Areas. Journal of Southern African Institute of Mining and Metallurgy. 2019; 119(11): 774-779. https://doi.org/10.17159/2411-9717/415/2019
[25] Lu Q, Qiao J, Peng J, Liu Z, Liu C, Tian L and Zhao J. A typical Earth Fissure Resulting from Loess Collapse on the Loess Plateau in the Weihe Basin, China. Engineering Geology. 2019; 259 (1): 832-837. https://dx.doi.org/10.1016/j.enggeo.2019.105139.
[26] Liu C, Yu Z, Zhan J, Wu M, Sun Y and Peng J. Damaging Effects of Earth Fissures in High-Speed Railway Bridges: Insights from Physical Experiments and Numerical Simulations. Transportation Geotechnics. 2024; 45(1): 556-559. https://dx.doi.org/10.1016/j.trgeo.2024.101182
[27] Zhu Z, Jiang M, Yu S and Li Y. Cracking Mechanism of Fissure-hole Specimens under Compression-Shear Conditions: Insights from Sand 3D Printing Technology and DEM Simulations. Theoretical and Applied Fracture Mechanics. 2025; 139(1): 532-555. https://dx.doi.org/10.1016/jtafmec.2025.105017
[28] Pelekis P, Batilees A, Lainas S, and Depountis N. The Influence of Pre-existing Tension Cracks on the Stability of Unsupported Temporary Excavations in Stratified Hard-clays: a case study of Corfu Island, Northwestern Greece. MDPI Journal of Geosciences. 2025; 15(5): 187-195. https://dx.doi.org/10.3390/geosciences/5050187
[29] Ozer M, Ulusay R, and Isik NS. Evaluation of Damage to Light structures Erected on a Fill Natural Rich in Expansive Soil. Bulletin of Engineering Geology and Environment. 2012; 71(1): 21-36. https://doi.org/10.1007/s10064-011-0395-2
[30] GH. Geophex Report. Mechanical Soil Stabilization Erosion Control System on Mine Sites. Geohex Report Bulletin, 2020; 11
[31] Al-Subari L, Hanafi M, and Ekcinci A. Effects of Geosynthetic Reinforcement on the Bearing Capacity of Strip Footing on Sandy Soil. SN Applied Sciences, 2020; 2(1): 1484. https://doi.org/10.1007/s42452-020-03261-5
[32] Seulveda SA, Pastern C, Moya S, Garcia M, Lara M, Montalva GA, Quiroz J, Hermanns, RL, Molina FY, Oppikofer T and Penna I. 2016. Site Investigation and Modelling Earthquake-Induced Rockslides in Central-Southern Chile. In Book. Landslides and Engineered Slopes. Experience, Theory and Practice. https://dx.doi.org/10.1201/b21520-227
[33] Zhang YZ, Wu, X, Zhang X, and Mei AS. Permeabiliy Characteristics of Bedrock Fissures under Disturbance Conditions Based on Neural Network. Neural Computing and Applications Journal, 2021; 33 (1): 4041-4051. https://dx.doi.org/10.1038/s41598-025-01036-9
[34] Okewale IA and Grobler H. Inherent Complexities in Weathered Rocks; a case of Volcanic Rocks, 2021; 54(1): 5533-5554. https://doi.org/10.1007/s00603-021-02569-x
[35] Ademola O. Pre-foundation Geophysical Investigation of a Site for Structural Development in Oke, Nigeria. NRIAG Journal of Astronomy and Geophysics. 2022; 11(1): 45. https://.doi.org/10.1080/20909977.2021.1953297
[36] Garleh AS and Shakir H. Effects of Bedrock Ridges in Formation of Earth Fissures due to Laid Subsidence. Bulletin of Engineering Geology and the Environment, 2022; 81(1): 23-27. https://doi.org/10.1007/s10064-022-02952-0
[37] Zhang Y, Wang Y, Shar KF and Li T. Moisture Stabilization of Embankment Sub-Grade with Capillary Barrier Cover under Dry and Rainy Weathers. Transportation Geotechnics. 2023; 42(1): 1134-1138. https://doi.org/10.1016/j.trgeo.2023.101057
[38] Ouslimane N, Barebita H, and Belfaquir M. Recovery and Valorization of Crushed Concrete and Glass waste in Road Construction in Morocco. Innovative Infrastructure Solutions, 2023; 8(239): 345-352. https://doi.org/10.1007/s41062-023-01198-3
[39] Adenika CI, Anyibi EA, Awoyemi MO, Adebayo AS, Dasho OA and Olagunju EO. Application of Geophysical Approach to Highway Pavement, Failure. A Case Study of the Basement Complex terrain, Southwestern Nigeria. International Journal of Geo-engineering, 2018; 9(8): 212-223. https://doi.org/10.1186/s40703-018-0076-0
[40] Lee S. Mastery Reinforced Earth for Foundation Projects. Design, Construction and Maintenance. ASIP Reliability, 2025; 72.

[41] Peng C, Du X, Liu W, and Huang B. 2025. Experimental and Simulation Study of Fissure and Hole Effect on Sandstone Failure. Environmental Earth Sciences. 75(8): 777-785. https://dx.doi.org/10.1006/j.aej.2025.01.100.
[42] Li W. Research Progress and Future Work on Earth Fissures in Su-Xi-Chang area. Earth. 2015; 5(1): 372-374.
[43] Wang GY, You G, Zhu J, Li W. Earth Fissures in Su-Xi- Cgang Region, Jiangsu, China. Surveys in Geophysics, 2016; 37(6): 1095-1116.
[44] Phogat VS, Singhal A, Mittal RK, and Singh AP. The Impact of Construction of Hill Roads on the Environment Assessed using the Multi-Criteria Approach. International Journal of Environmental Studies. 2022; 79(1): 101-104.
[45] Bayode S and Akpaorebe O. An Integrated Geophysical Investigation of a Spring in Ibuji, Igbara-Oke, Southwestern Nigeria. Ife Journal of Science, 2011; 13(1): 63-74.
[46] Onoja SO and Osifila, OJ. Integrated Geophysical Investigation of a Suspected Spring in Igbokoran, Ikare-Akoko, Southwestern Nigeria. IOSR Journal of Applied Geology and Geophysics, 2015; 3(5): 83-91.
[47] Carreon-Freyre D, Cerca M, Ochoa-Gonzales G, Teatini P, Zuniga FR. 2016. Shearing along Faults and Stratigraphic Joints controlled by Land Subsidence and Hydraulic Gradients in the Valley of Queretaro, Mexico. Hydrogeology Journal. 24(3): 657-674.
[48] Mandal A and Mishra U. Integrated Geophysical Investigation to Map Shallow Surface Alteration/Fracture Zones of Atri and Tarabalo Hot Springs, Odisha, India. Geothermics, 2019; 77(1): 24-33
[49] Obiadi, II, Onwuemes, AG, Anike OL, Obiadi, CM, Ajaegwu, NE, Anakwuba EK, Akpunonu EO, and Ezim EO. Imaging Subsurface Fracture Characteristics using 2D Electrical Resistivity Tomography. International Research Journal of Engineering Science, Technology and Innovation, 2012; 1(4): 103-110.
[50] Al-Fares W, and Asfahani J. Evaluation of the Leakage Origin of Abu-Baara Earthen Dam using Electrical Resistivity Tomography, Northwestern Syria. Geofisica Internationa. 2018; 57(1): 223-237.
[51] Olorunfemi MO, Oni AG, Bamidele OE, Fadare TK and Aniko OO. Combined Geophysical Investigations of the Characteristics of a Regional Fault Zone for Groundwater Development in a Basement Complex Terrain of Southwestern Nigeria. Discover Applied Water Sciences, 2020; 2(103): 666.
[52] Sangodiji EE and Olorunfemi MO. Geophysical Investigation of a Suspected Foundation Failure at Ogbomoso, Southwestern Nigeria. Pacific Journal of Science and Technology, 2013; 14(2): 522-536.
[53] Ibitoye FP, Ipinmoroti FV, Salami M, Akinluwade KJ, Taiwo AT, Adetunji AR. Application of Geophysical Methods to Buildingh Foundation Studies. International Journal of Geosciences, 2013. 4(1): 1256-1266. https://dx.doi.org/10.4236/ijg.2013.49120
[54] Pang JB, Huang QB, Hiu ZP, Wang, MX, Li T, Men YM, Fan W. A Proposed Solution to the Ground Fissures Encountered in Urban Metro Construction in Xian China. Tunneling and Underground Space Technology, 2017; 61(1): 12-25. https://dx.doi.org/10.1016/j.tust.2016.09.002
[55] Canada M. Faulty designs: Lessons from the Failures of the Past. Menard Group News. 2024. https://quizlet.com/324263565/geotechnical-engineering-flash-cards/.
[56] Rafferty JP 2012. Earth Sciences Geologic Time and Fossils. Earth Sciences. 226.
[57] Shu, B and Ma, B. Study of Ground Collapse Induced by Large-Diameter Horizontal Directional Drilling in a Sand Layer using Numerical Modelling . Canadian Geotechnical Journal, 2015; 52(10): 1562-1574. https://dx.doi.org/10.1139/cgi-2014-0388.
[58] Adcock D. Geotech Failure and Lesson Learned; Case Studies. Monitoring Geotech Newsletter, 2023:1-21.
[59] Adcock D. 2024. Seven Forces shaping Geotechnical Engineering in 2024. Monitoring Geotech Newsletter. 15-38.
[60] Lees A. Home Geotechnical Settlement: Types and How They Work. Tensar International Limited Blackburn, United Kingdom. Tensar Bulletin, 2025 .
[61] Oyinloye AO. Geology and Geotectonic setting of the basement complex rocks in South Western Nigeria implications on provenance and Evolution, Earth and Environmental Sciences. 2011; 5.
[62] Bayewu OO, Oloruntola MO, Mosuro GO, Folorunso IO, and Kolawole, AU. Evaluation of Resistivity Anisotropy of Parts of Ijebu Igbo, Southwestern, Nigeria Using Azimuthal Resistivity Survey (ARS) Method. Journal of Geography and Geology, 2014; 6 (4):140-152

[63] Onakomaiya SO Oyesiku K, and Jegede FJ. Ogun State in Maps. Rex Charles Publications, 1992; 128.
[64] Akanni CO. 1992. Aspects of Climate. In: Ogun State in Maps, Onakomaya, SO, Oyesiku K and Jegede J. (Eds.). Rex Charles Publication, Ibadan, Nigeria. 207.
[65] Adekoya SA, Coker JO Adenuga OO. 2017. Characterization of Aquifer Using Geostatistical Analysis of the Geoelectrical Parameters of Ijebu Igbo South-West Nigeria. Journal of Scientific and Engineering Research, 2017, 4(7): 74-81.
[66] Ishola SA and Olufemi ST. Groundwater Exploration using Geoelectric Technique in Oru-Ijebu, South-West Nigeria. Nigerian Journal of Theoretical and Environmental Physics, 2024; 2(1): 49-66. https://doi.org/10.62292/njtep.v2i1.202420.
[67] Jones HA, and Hockey RD. The Geology of Parts of Southwestern Nigeria. Geological Survey of Nigeria Bulletin, 1964; 31(1): 22 – 24.
[68] Hassan M, Shang Y, Jin. W. Delineation of Weathered Fracture Zones for Aquifer using Integrated Geological Approach. A case study from South China. Journal of Applied Geophysics, 2018; 157(1): 47-60. http://doi.org/10.1016/j.jappgeo.2018.06.017
[69] Rahaman MA. A review of the Basement Complex Geology of Southwestern Nigeria. In Geology of Nigeria (edited by C.A. Kogbe, C.A) Elizabethan publishing company, Lagos, 1976; 41-58.
[70] Obaje NG. Geology and Mineral Resources of Nigeria. Springer Berlin Heidelberg, 2009; 120(1): 23-28. https://doi.org/10.1007/978-3-540-92685-6
[71] Griffiths DH and Barker RD. Two-Dimensional Resistivity Imaging and Modeling in Areas of Complex Geology. Journal of Applied Geophysics, 1993; 29(1):211- 226 https://doi.org/10.1016/0926-9851(93)90005-J
[72] Aizebeokhai AP, Olayinka AI, Singh VS. Application of 2D and 3D geoelectrical Resistivity Imaging for Engineering Site Investigation in a Crystalline Basement Terrain, Southwestern Nigeria. Environ Earth Science, 2010; 61(7):1481–1492. https://doi.org/10.1007/s12665-010-0474
[73] Loke, MH. 2003. Tutorial of 2D and 3D Electrical Imaging Surveys for Environmental and Engineering Studies. https://sites.ualberta.ca/~unsworth/UA-classes/223/loke_course_notes.pdf
[74] Zhang D. Influences of Deep Foundation Pit Excavation in the Stability of Adjacent Building. Special Issues of Advances in Structural Monitoring for infrastructures in Construction. MPDI Buildings. 2004; 13(80): 172. 196. https://dx.doi.org/10.3390/buildngs13082004
[75] Akinlabi IA and Bayowa OG. 2D Electrical Resistivity Imaging of Bedrock Fissures in Ogbomoso, Southwestern Nigeria. LAUTECH Journal of Civil and Environmental Studies, 2021; 7(2): 46-54. https://dx.doi.org/10.36108/laujoces/120270.0250
[76] Lachassagne P, Dewandel B and Wyns R. Hydrogeology of Weathered Crystalline/Hard-rock Aquifers-Guidelines for Operational Survey and Management of their Groundwater Reserves. Hydrogeology Journal, 2021; 29(1): 2561-2594. https://doi.org/10.1007/s10040-021-02339-7
[77] Turgrul A. Effect of Weathering on Pore Geometry and Compressive Strength of elected Rock Types from Turkey. Engineering Geology, 2004; 25(3-4): 215-227. https://doi.org/10.1016/enggeo.2004.05.008.
[78] Briski M, Stroj A, Kosovic I, and Borovic S. Characterization of aquifers in Metamorphic Rocks by Combined use of Electrical Resistivity Tomography and Monitoring of Spring of Hydrodynamics. Geosciences, 2020; 10(4): 137. https://.doi.org/10.3390/geosciences10040137
[79] Gao Q, Shang, Y, Hassan, M, Jin, W and Yang P. Evaluation of a Weathered Rock Aquifer using ERT Method in SouthGuangdona, China. Water Journal, 2018; 10(3): 293. https://doi.org/10.3390/w10030293
[80] Ye S, Wang Y, Wu J., Teatini P, Yu J, and Gong X. Characterization of Earth Fissures in South Jangu, China. Proceedings of the International Association of Hydrological Sciences, 2015; 372(1): 249-253. https://doi.org/10.5194/piahs-372-249-2015
[81] Edunjobi HO, Layade GO, Falufosi, MO and Olurin OT. Lineament and Depth Evaluation of Magnetic Sources in a Geological Transition Zone of Abeokuta and its Environs, Petroleum and Coal, 2021; 63(2): 548-560

To whom correspondence should be addressed: Sakirudeen Akinola Ishola, Department of Earth Sciences, Olabisi Onabanjo University Ago-Iwoye, P.M.B 2002, Ago-Iwoye, Ogun State, Nigeria,
E-mail: ishola.sakirudeen@pouagoiwoye.edu.ng